This is an *Accepted Manuscript*, which has been through the Royal Society of Chemistry peer review process and has been accepted for publication.

Accepted Manuscripts are published online shortly after acceptance, before technical editing, formatting and proof reading. Using this free service, authors can make their results available to the community, in citable form, before we publish the edited article. We will replace this *Accepted Manuscript* with the edited and formatted *Advance Article* as soon as it is available.

You can find more information about *Accepted Manuscripts* in the **Information for Authors**.

ROYAL SOCIETY OF CHEMISTRY

www.rsc.org/dalton

ION EXCHANGE AND INTERCALATION PROPERTIES OF LAYERED DOUBLE HYDROXIDES TOWARDS HALIDE ANIONS

Umberto Costantino[a], Riccardo Vivani[b], Maria Bastianini[a], Ferdinando Costantino[a] and Morena Nocchetti*[b]

[a]*Dipartimento di Chimica, Biologia e Biotecnologie, Università di Perugia, Via Elce di Sotto, 8,*

Perugia, 06123 - ITALY

[b]*Dipartimento di Scienze Farmaceutiche, Università di Perugia, Via del Liceo, 1, Perugia, 06123 -*

ITALY

ABSTRACT

A layered double hydroxide (LDH) obtained by the urea method, having empirical formula $[Zn_{0.61}Al_{0.39}(OH)_2](CO_3)_{0.195} \cdot 0.50H_2O$, has been converted into the corresponding chloride form $[Zn_{0.61}Al_{0.39}(OH)_2]Cl_{0.39} \cdot 0.47H_2O$ by contacting the solid with a proper HCl solution. The intercalation of the other halide anions ($X^- = F^-$, Br^-, I^-) *via* the Cl^-/X^- anion exchange has been attained and the respective anion exchange isotherms have been obtained with the batch method. The analysis of the isotherms indicates that the selectivity of LDH towards the halides decreases with the increase of the X^- ionic radius, the selectivity order being $F^- > Cl^- \geq Br^- > I^-$. The CO_3^{2-}/Cl^- isotherm has been also reported to highlight the extraordinary selectivity of LDH towards carbonate anions. Samples taken from the isotherms at different exchange degrees were analyzed by X-ray diffraction, thermogravimetry and thermodiffractometry to obtain information about the ion exchange mechanism. The Cl^-/Br^- and the reverse Br^-/Cl^- exchanges occur with the formation of solid solutions, very likely because of the similar ionic radius of the exchanging anions. Differently, in the Cl^-/F^- and Cl^-/I^- exchange, the co-existence in the same sample of the Cl^- and F^- (or I^-) phases were detected, indicating the occurrence of a first order phase transition, in which the starting phase is transformed into the final phase, as the process goes on. The variation of the interlayer distances of ZnAl-X intercalation compounds with the hydration degree has been interpreted with a structural model based on the nesting of the guests species into the trigonal pockets of the brucite-like layer surface. Rietveld refinements of the phases with the maximum F^-, Br^- and I^- content were also

performed and compared with the above model, giving indications on the arrangement and order/disorder of the halide anions in the interlayer region.

INTRODUCTION

Among the layered solids capable of intercalation the layered double hydroxides (LDH) have a special role because of their structural and compositional features, their simple and inexpensive preparation methods and because they are rare examples of layered solids with positively charged layers balanced by exchangeable anions.[1] They are represented by the general formula $[M(II)_{1-x}M(III)_x(OH)_2][A_{x/n} \cdot zH_2O]$, where M(II) is typically Mg, Zn, Ni, Cu; M(III) can be Al, Fe, Cr. A is an anion with charge n^- like CO_3, SO_4, Cl or other inorganic or organic anion and z is the mol of co-intercalated water per formula weight. The isomorphic substitution of M(II) with M(III) cations in the brucite-like sheet produces positive electric charges balanced by the exchangeable anion and determines the x value that generally ranges between 0.2 and 0.4. The x value indeed determines the charge density of the layers and hence the anion exchange capacity of the solid. The brucite-like layers are constituted of edge sharing octahedra, the centres of which are occupied by metal cations and the vertices by hydroxide ions.[2]

At present, LDH-based compounds form a large class of materials widely used as catalysts,[3] additives for polymers,[4] anion exchangers, hosts for storage and release of species with biological activity.[5]

Despite the vast literature on these layered materials, fundamental and systematic studies dealing with the layer rigidity, ion exchange mechanism and the anion selectivity are not exhaustive. The first selectivity scale was reported by Miyata in 1983;[6] more recently Nenoff et al. proposed a selectivity scale toward monovalent anions and demonstrated that it was independent of the LDH method of synthesis.[7] The poor information available induced our research group to undertake a program to deep the knowledge on these topics. Previous studies were performed to assess the layer rigidity of LDH[8] since the intercalation mechanism is affected by this parameter. The "discrete finite layer rigidity" model developed by Solin was applied on a Zn-Al LDH in chloride form. This model allows to determine a parameter (p), that is related to the area of the lamella that is not puckered during an ion exchange and intercalation process: the higher is p, the more rigid is the lamellae. Solids having flexible lamellae, as graphite, give intercalation reactions by staging or with the formation of a phase boundary between the two immiscible phases of the outcoming and the incoming ions, with a first order phase transition.[9,10] On the other hand, in a rigid material the intercalation may occur either by the formation of a solid solution or by staging depending on the dimension of the guest species.[10] The p parameter found for LDH, places them halfway between

flexible and rigid materials, suggesting that in these solids the intercalation process may occur with different mechanisms, also depending on the reciprocal size of the involved anions. Previous works showed that the intercalation of several carboxylates[11] or phosphonates[12] produced 2-stage intercalation compounds, while the CO_3^{2-}/Cl^- exchange can occur through a 1st order phase transition mechanism or even with the formation of a solid solution.[8]

This work aimed to study the selectivity of the ZnAl-LDH in chloride form towards halides ($X^- = F^-$, Br^-, I^-) performing ion exchange isotherms Cl^-/X^-. The mechanism of these ion exchange processes was studied analyzing each point of the isotherms by X-ray diffraction and Rietveld refinement of the LDH containing the maximum amount of F^-, Br^- and I^-. The effect of the hydration water and of the anion dimensions on the interlayer distance was also investigated.

EXPERIMENTAL

Materials

All the chemicals used in this work were C. Erba RP-ACS products.

Preparation of halide-LDH derivatives

The LDH with formula $[Zn_{0.61}Al_{0.39}(OH)_2](CO_3)_{0.195} \cdot 0.5H_2O$ (ZnAl-CO_3), was synthesized using the urea method.[13] The corresponding chloride form, with formula $[Zn_{0.61}Al_{0.39}(OH)_2]Cl_{0.39} \cdot 0.47H_2O$ (ZnAl-Cl) was obtained by titrating 5 g of carbonate form, dispersed in 50 ml of 0.1 M NaCl solution, with a 0.1 M HCl by means of Radiometer automatic titrator operating at pH stat mode, and pH value of 5.

The forward ion exchange isotherms were obtained equilibrating weighed amount of ZnAl-Cl with increasing volumes of 0.1 M of NaX aqueous solution ($X = F^-$, Br^-, I^-) for 7 days (sample obtained labeled as: ZnAl-F, ZnAl-Br, ZnAl-I). The reverse Br^-/Cl^- isotherm was performed as above described starting from $[Zn_{0.61}Al_{0.39}(OH)_2]Br_{0.39} \cdot 0.52H_2O$ (ZnAl-Br) as exchanger and 0.1 M of NaCl aqueous solution. The isotherms were obtained plotting the ionic fraction of the X in the solid vs the ionic fraction of X in the solution (mequiv. X^-/(mequiv. X^- + mequiv. Cl^-)).

The Cl^-/CO_3^{2-} isotherm was performed equilibrating weighed amount of ZnAl-Cl with calculated volumes of 0.05 M Na_2CO_3 aqueous solution for 3 days. Pure ZnAl-Br was obtained by titration of the carbonate form with 0.1 M HBr, after dispersing the carbonate form in 0.1 M NaBr solution at constant pH of 5. The isotherm was obtained plotting the ionic fraction of the CO_3^{2-} in the solid vs the ionic fraction of CO_3^{2-} in the solution (mequiv CO_3^{2-} / (mequiv CO_3^{2-} + mequiv Cl^-)).

Details of the experimental part are reported in the SI.

The recovered solids were washed three times with CO_2-free de-ionized water, dried at 75% relative humidity (RH) and characterized by ion chromatography, XRPD taken at different temperatures and TG analyses.

Analytical procedures.

Zn and Al contents were obtained by Inductively Coupled Plasma Spectroscopy after having dissolved a weighed amount of sample (~20 mg) in few drops of concentrated HNO_3 and properly diluted with water. Halide contents were obtained by ion-chromatography both on the mother liquor of the isotherms and on the solid. In the latter case, a given amount of sample (~100 mg) was equilibrated in 20 ml of Na_2CO_3 1 M solution for 12 h in order to extract all halides from the solid. The solution was then analyzed by ion chromatography. Hydration water and carbonate content of the solids were obtained by thermogravimetry. This technique allowed to confirm also the halide contents.

Instrumentation

Elemental analyses were performed by Varian 700-ES series Inductively Coupled Plasma-Optical Emission Spectroscopy (ICP-OES).

X-ray diffraction patterns were collected with the $CuK\alpha_{1,2}$ radiation with a α1/α2 ratio of 0.5 (1.5424 Å) on a Philips X′Pert Pro diffractometer, equipped with the X′Celerator solid state fast detector with a 0.017° step size and 30 s per step counting time. Thermodiffractometric analysis was performed under air with an Anton Paar HTK 1200N hot chamber mounted on a Philips XPERT APD 3020 diffractometer in the 25−200 °C temperature range. Thermogravimetric analysis was performed with a Netzsch STA 449 C Jupiter (thermal analyzer) at a heating rate of 5°/min under an air flow.

The ion-chromatography analysis was performed using a Dionex 2000 equipped with an ionic conductivity detector. The extracted F^- anions were detected using a column AS4A, $NaHCO_3$ 3.5 mM as eluent and H_2SO_4 12.5 mM as suppressor for the ionic conductivity detector. The other extracted halides were detected using the same conditions used for the fluoride anions except for the eluent that was $NaHCO_3$ 1.7 mM and Na_2CO_3 1.8 mM.

Coupled thermogravimetric (TG) and differential thermal analyses (DTA) were performed by a thermal analyzer (STA 449C Jupiter, Germany) in air flow of 30 ml/min and heating rate of 10°C/min to determine the weight loss as a function of temperature.

Rietveld refinement of the F⁻ and Br⁻ exchanged LDH

The refined structures of ZnAl-Cl and ZnAl-I have been already reported in literature.[14] Herein we report the refined structures of the ZnAl-F and ZnAl-Br forms. Structural and refinement details are reported in Table 1.

The samples were carefully side-loaded into a zero-background quartz sample holder in order to avoid preferred orientation.

Rietveld refinement was carried out by using the GSAS program. A Pseudo-Voigt profile function TCHZ (profile function n. 3)[15] has been used and 7 terms (included two terms for the modelling of the asymmetry at low 2θ angles) have been also refined. A March-Dollase model was used in order to refine the preferred orientation of the basal *00l* planes. The M-OH distance was refined by restraining the z coordinate of the hydroxyl OH group to about 2.0(5) Å, while the thermal factors of the interlayer species (X⁻ and oxygen atoms of water molecules) were also refined at the same value by constraining the program to apply the same shift.

Table 1 Crystal data and refinement details for ZnAl-X (X = Cl⁻, F⁻, Br⁻, I⁻)

	ZnAl-Cl [ref. 14b]	ZnAl-F [this work]	ZnAl-Br [this work]	ZnAl-I [ref. 14a]
Space group	*R* -3*m*	*R* -3*m*	*R* -3*m*	*R* -3*m*
a/Å	3.0749(6)	3.0738(1)	3.0835(1)	3.0807(1)
c/Å	23.1524(5)	22.5638(5)	23.687(1)	24.3941(4)
V/Å^3	189.58(6)	184.64(1)	195.05(1)	200.50(1)
Z	3	3	3	3
Rwp	0.119	0.110	0.076	0.067
Rp	0.088	0.085	0.057	0.046
R$_{F2}$	0.076	0.050	0.074	0.103
GOF	4.7	6.2	2.7	3.8

$Rp = \Sigma|Io - Ic| / \Sigma Io.$
$Rwp = \{\Sigma[w(Io - Ic)^2] / \Sigma[wIo^2]\}^{1/2}$
$R_{F2} = \Sigma|Fo^2 - Fc^2| / \Sigma|Fo^2|$
$GOF = \{\Sigma[w(Io - Ic)^2] / (No - Nvar)\}^{1/2}$

RESULTS AND DISCUSSION

Ion exchange isotherms and mechanism

Carbonate anions, because of their geometry and their bivalent nature, are strongly held in the interlayer region and it is very difficult to replace them with other anions using a simple ion-

exchange process. A method to prepare an LDH containing an easily exchangeable anion, such as Cl⁻, involved the treatment of ZnAl-CO₃ with hydrochloric acid, which reacted with the carbonate anions and produced carbon dioxide, water and LDH in chloride form. The intercalation of other halides was achieved by ion exchange starting from ZnAl-Cl. Before studying the LDH halide systems, the Cl⁻/CO₃²⁻ ion-exchange isotherm obtained at 25°C and ionic concentration of 0.05 M has been studied in order to get information on this ion-exchange mechanism. The isotherm, shown in Fig. 1, is completely shifted to the left side, and about all the added carbonates are uptaken by the solid up to a CO₃²⁻ ionic fraction in the solid equal to 0.31. Additional carbonate uptake requires a small increase of CO₃²⁻ ionic fraction in solution (mequiv CO_3^{2-} / (mequiv CO_3^{2-} + mequiv Cl⁻)).
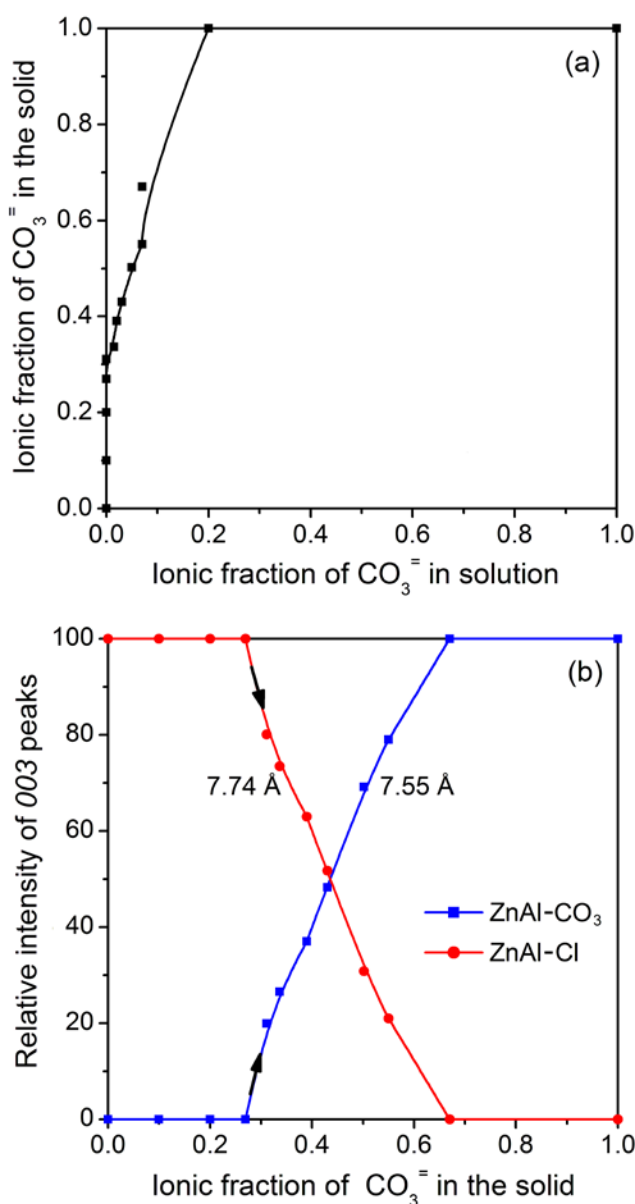
Fig. 1 (a) Cl⁻/CO₃²⁻ ion-exchange isotherm obtained from [Zn₀.₆₁Al₀.₃₉(OH)₂]Cl₀.₃₉·0.47H₂O and 0.05 M Na₂CO₃ (pH = 10.9), at room temperature. (b) Percentage of the carbonate and chloride phases in the ZnAl-Cl/CO₃ systems as a function of ionic fraction of the carbonate in the solid.

6

XRPD patterns of the samples at different CO_3^{2-} content show that the ion exchange process takes place through three well differentiated steps. These steps can be described by plotting the relative intensity, assumed proportional to the relative amount of phases, of the *003* diffraction maxima of the carbonate and of the chloride phase, as a function of carbonate ionic fraction in the solid (Fig. 1(b)). It can be seen that in the range 0-27% of exchange a single phase is present, suggesting the formation of a solid solution of carbonate into the chloride phase. In the range 27-67% of exchange two immiscible phases of approximate composition $[Zn_{0.61}Al_{0.39}(OH)_2](CO_3)_{0.052}Cl_{0.285} \cdot zH_2O$ and $[Zn_{0.61}Al_{0.39}(OH)_2](CO_3)_{0.13}Cl_{0.13} \cdot zH_2O$ respectively, are present. As the exchange proceeds the first phase is transformed into the second phase. From 67 to 100% of CO_3^{2-} uptake another solid solution is formed, where chloride is solubilised into the carbonate phase.

The Cl^-/Br^- forward and reverse isotherms are shown in Fig. 2. These two anions involved in the exchange process have similar anionic radii ($r_{Cl^-} = 1.81$Å, $r_{Br^-} = 1.96$Å).[16] The obtained isotherms resemble to those of an exchanger resin with equivalent sites and without phase separation.
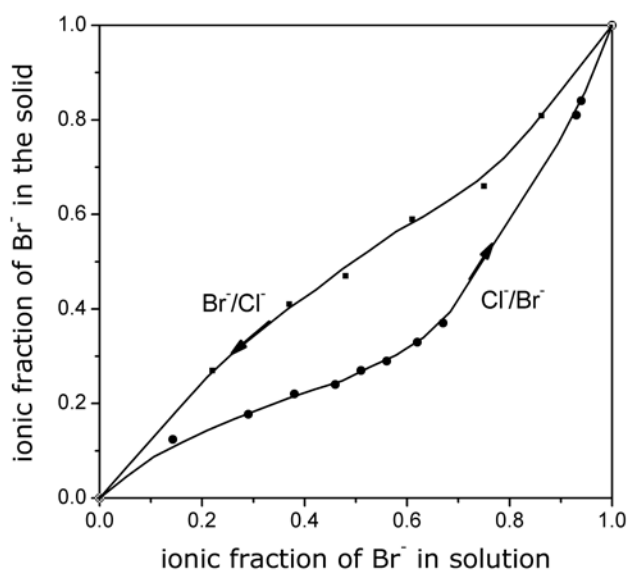
Fig. 2 Forward and reverse isotherms of the Cl^-/Br^- ion exchange process.

The isotherms show an hysteresis loop meaning that, at the same composition of the solution, two solid phases with different content of chloride and bromide may be present depending on whether the starting phase is ZnAl-Cl or ZnAl-Br.

The forward isotherm is positively curved and falls below the diagonal proving that the chloride is preferred. On the other hand, the reverse isotherm is S-shaped, assessing that the relative affinity for the incoming chloride decreases when the conversion degree increases.

7

Fig. 3a and 3b show the *006* reflections of the XRPD of selected members of the forward and reverse isotherms. Separate considerations are required. The *006* reflection of forward isotherm samples, in which chloride is replaced by the bigger bromide, shifts at lower angles in the range 0-37% of exchange. In this range a single phase is present and the ion exchange seems to proceed with the formation of a solid solution in which the bromide and chloride are solubilized in the same phase. A slight increment of the bromide ionic fraction in the solution leads to a substantial increase in the bromide ionic fraction in the solid, as shown by the increased slope of the isotherm. The sample containing 84% of bromide is constituted by two immiscible phases: the pure bromide phase (d = 7.85Å) and a phase with intermediate interlayer distance between bromide and chloride phases (d = 7.80Å), that presumably contains both bromide and chloride. As the exchange proceeds the latter phase is transformed into the bromide phase. From 84% to 100% of bromide uptake the ion exchange seems to proceed by a first order phase transition from the intermediate phase with d = 7.80Å to the pure bromide phase.

In the reverse isotherm, when bromide is replaced by the smaller chloride, a gradual shift of the *006* reflection from the chloride to the bromide phases is observed: the ion exchange seems to go on with the formation of a solid solution in which chloride is solubilised into the bromide phase.
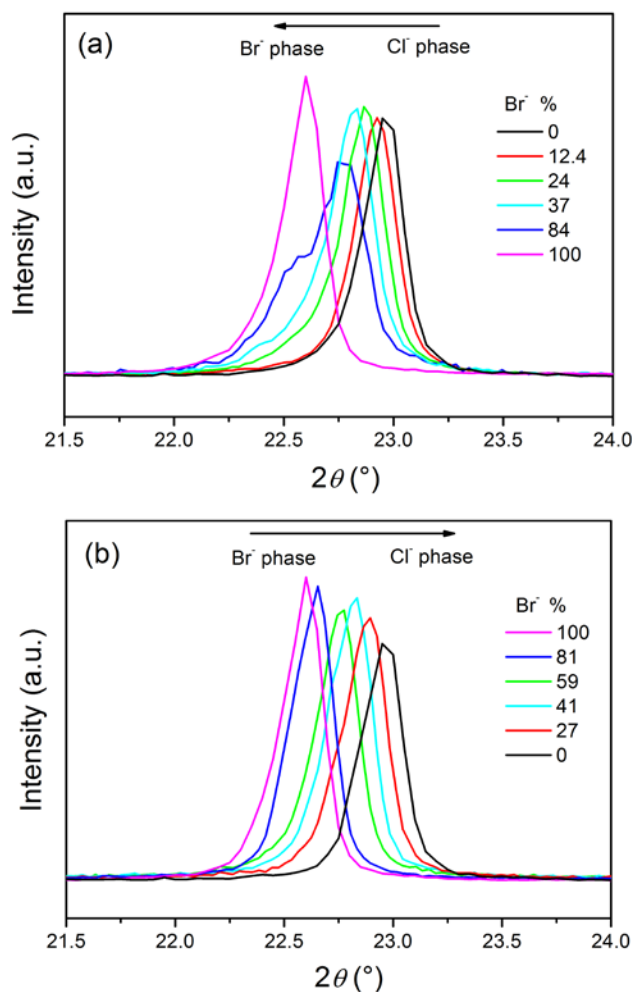
Fig. 3 *006* reflections of the XRPD of selected members of the forward (a) and reverse (b) Cl⁻/Br⁻ isotherms.

In Fig. 4 the Cl⁻/Br⁻ ion exchange isotherm is compared with those obtained exchanging the chloride with the smaller fluoride and with the bigger iodide.
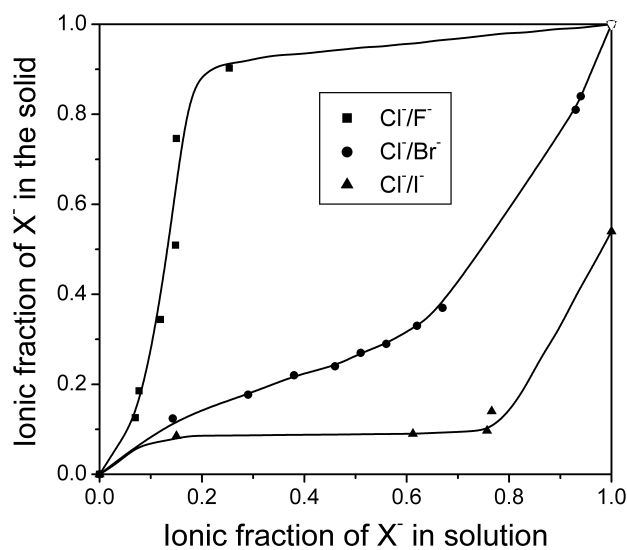
Fig. 4 Forward Cl$^-$/F$^-$, Cl$^-$/Br$^-$ Cl$^-$/I$^-$ ion exchange isotherms.

The selectivity of LDH towards halides is clearly affected by the anion sizes. LDH shows a high selectivity towards fluoride, whose ionic radius (1.33 Å) is about 0.5 Å smaller than that of chloride. On the contrary, LDH shows a low affinity for iodide which has a ionic radius (2.20 Å) about 0.4 Å bigger than chloride. Therefore by the analysis of the isotherm positions it is possible to determine the following selectivity order: F$^-$ > Cl$^-$ ≥ Br$^-$ > I$^-$.

The preparation of fully exchanged phases strongly depends on the above selectivity scale: fluoride was able to completely exchange chloride by simply contacting ZnAl-Cl with a 0.1 NaF solution; to obtain the pure bromide phase, the ion-exchange reaction was forced by titrating ZnAl-Cl with 0.1 M HBr, while the conversion of the LDH into the iodide form did not exceed the 54% of its ion exchange capacity.

The above selectivity scale can be explained considering a simple model. During the ion exchange process the incoming ion moves from the solution to a fix charge of the host and the outcoming ion leaves the lattice position to diffuse into the solution. The standard Gibbs energy variation associated to the anion/chloride exchange depends on: a) the electrostatic interactions between the positive charges of the lamellae and the negative charges of the anions; b) the standard Gibbs energy associated to the different anions, that can be approximated to the hydration enthalpy neglecting the entropy contributions. It can be formulated as:

$$\Delta G°_{anion/Cl^-} = \left(\frac{e^2}{r_{fix} + r_{Cl^-}} - \frac{e^2}{r_{fix} + r_{anion}} \right) - \left(\Delta G°^{hydr.}_{Cl^-} - \Delta G°^{hydr.}_{anion} \right)$$

where r_{fix} is the fix charge radius, that is constant and equal to half of the lamella thickness, r_{anion} is the halide ion radius and $\Delta G°^{hydr}$ is the Gibbs energy variation associated to the anion hydration change.[17] The experimental selectivity scale suggests that electrostatic interactions between the layer and the guests and then the anion radii of the guest mainly affect the standard Gibbs energy variation according to G. Costa.[18]

Each member of the Cl$^-$/F$^-$, and Cl$^-$/I$^-$ isotherms were studied by XRPD to get information about the ion exchange mechanism. Fig. 5 and 6 show the *006* reflections of the XRPD of Cl$^-$/F$^-$ and Cl$^-$/I$^-$ isotherm samples, respectively.
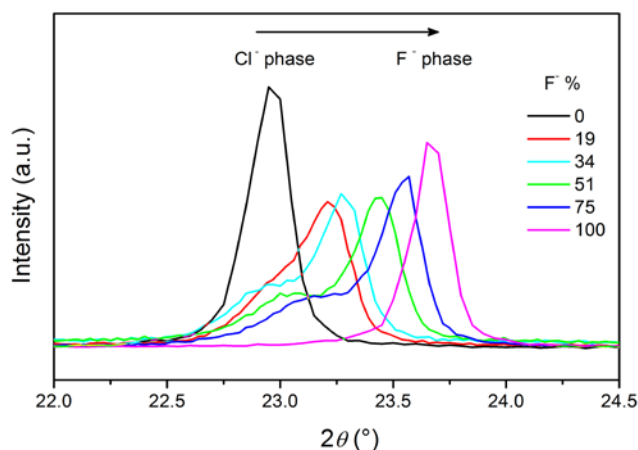
Fig. 5 *006* reflections of the XRPD of selected members of the Cl⁻/F⁻ isotherm.
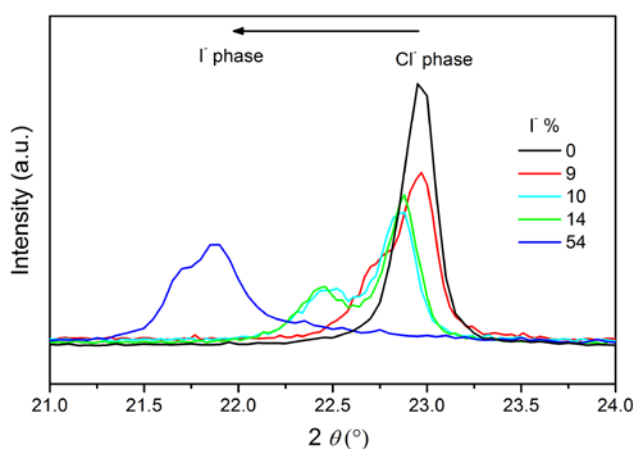
Fig. 6 *006* reflections of the XRPD of selected members of the Cl⁻/I⁻ isotherm.

The *006* reflection of the samples with an increasing amount of fluoride moves to higher diffraction angles, corresponding to smaller interlayer distances, in agreement with the smaller dimension of the fluoride anion (Fig. 5). On the contrary, samples with increased amount of iodide show a shift of the same peak to lower diffraction angles with respect to the starting chloride phase (Fig. 6). Note that each reflection is constituted by the convolution of two reflections: the *006* of the chloride phase and the *006* of the fluoride or iodide phase. The chloride phase converts into the fluoride or iodide phase during the ion exchange. The co-existence of the F⁻ (or I⁻) and Cl⁻ phases suggests that the ion exchange mechanism goes on by a first order phase transition.

Effect of the hydration on basal spacing of the halides-LDH phases

In Table 2 the empirical formulae, obtained from thermogravimetry and ion chromatography analyses, of ZnAl-X conditioned at 75% RH are reported. The basal spacings of the samples, when conditioned at 95% and 75% RH are also reported, and plotted versus the anionic radius in Fig. 7.

Table 2 The basal spacing of ZnAl-X conditioned at 95% and 75% RH.

Sample	$[Zn_{0.61}Al_{0.39}(OH)_2]Cl_mX_n \cdot zH_2O$			Basal spacing (Å)	
	m	n	$z*$	RH 95%	RH 75%
ZnAl-F	0	0.39	0.50	7.61	7.53
ZnAl-Cl	0.39	0	0.47	7.78	7.74
ZnAl-Br	0	0.39	0.52	7.88	7.85
ZnAl-I	0.18	0.21	0.34	11.2	8.14

*The water content refers to the sample dried at 75% RH.

The interlayer distance of the samples conditioned at 95% RH increases almost linearly as the anion radius increases except for I⁻ that exhibits a very high interlayer distance. A contraction of the basal spacing in a range of 0.03-0.08 Å was observed for ZnAl-F, ZnAl-Cl and ZnAl-Br conditioned at 75% RH; while the basal spacing of the iodide form, in the same conditions, lowers of 3.06 Å. According to Iyi et al.,[19] the increase of the basal spacing of 3.06 Å in ZnAl-I with a high hydration degree can be attributed to one additional water layer in the interlayer space, considering that the diameter of a water molecule is about 2.8 Å. The best linear correlation of the basal spacing of the samples conditioned at 75% RH was obtained by excluding ZnAl-F and giving the equation $d = 5.93 + 0.497 \times 2r$, where d is the basal spacing and r the ionic radius. The intercept value should represent the interlayer distance of LDH without anions in the interlayer region, that is the layer thickness; the best value of 5.93 Å differs significantly from the accepted value of 4.46 Å. This difference may be explained assuming that anions are not closely packed between adjacent layers, but they occupy more room, probably due to a certain level of disorder in the interlayer region. Hydration water, that share the same crystallographic site of the anion, may also contribute to this disorder.

The ZnAl-F basal spacing is higher than that predicted by the straight line in Fig. 7, because fluoride is the only anion of this series with a smaller diameter than the thickness of a water molecule. Therefore, only for ZnAl-F the basal spacing is determined by the hindrance of water molecule, and not the guest anion. The hindrance of water molecules in ZnAl-F is about 3 Å, calculated as the difference between the basal spacing reported in Table 2, and the thickness of an LDH layer.
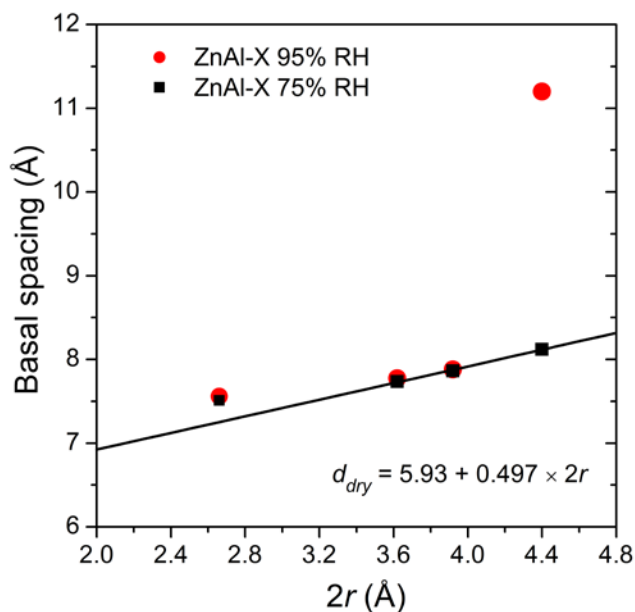
Fig. 7 Correlation between the basal spacing of ZnAl-X and ionic radius of the guest halide.

The hydration water molecules role on the basal spacings has been investigated collecting TG analysis (SI) and *in situ* high temperature XRPD patterns. As expected, all the samples undergo a contraction of the interlayer distance upon dehydration (Fig. 8). The basal spacing of ZnAl-X at increasing temperatures are reported in Table 3. It has been observed, from TG data, that the complete dehydration of the solids occurs at temperature of 150°C. Note that ZnAl-Cl, -Br, and -I are able to restore their hydrated forms when cooled in air.

Table 3 Basal spacing of ZnAl-X at different temperatures.

Sample	Basal spacing (Å)		
	100°C	125°C	150°C
ZnAl-F	7.53-6.77	7.28-6.50	6.30
ZnAl-Cl	7.51	7.42-7.3	7.30
ZnAl-Br	7.70	7.66	7.62
ZnAl-I	8.04	8.04	8.04
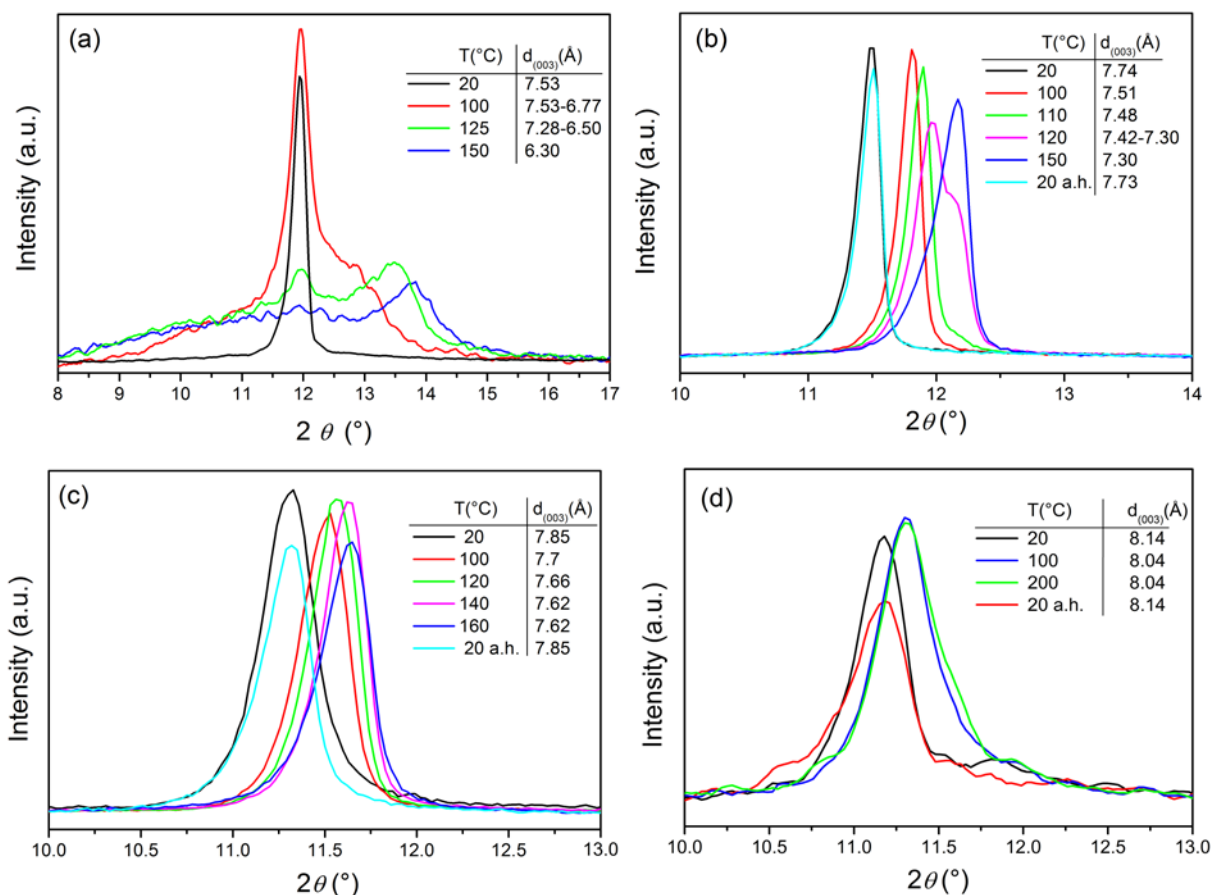
Fig. 8 XRPD patterns taken at the indicated temperatures of (a) ZnAl-F (b) ZnAl-Cl (c) ZnAl-Br (d) ZnAl-I samples. The basal spacings are also reported. a.h. = after heating.

Fig. 9 shows the dependence of basal spacings of samples dried at 150°C on the anionic diameter. A good linear correlation of the experimental data is obtained. The intercept on the y axis at diameter zero of the guest species should be the interlayer distance of the LDH without intercalated anions, hence the thickness of the layers. The obtained value (3.63 Å) is lower than the accepted value of 4.46 Å. Moreover, the experimental basal spacing of each sample is lower than that calculated with the equation $d = 4.46 + 2r$ (where 4.46 is the lamella thickness and r the ionic radius).
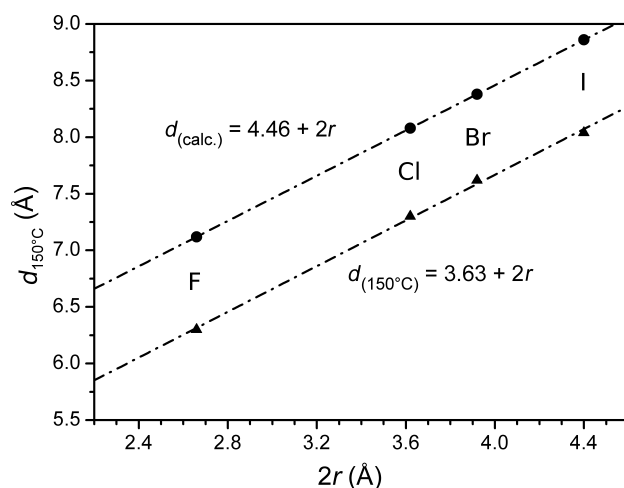
Fig. 9 Basal spacing of ZnAl-X dried at 150°C as a function of the anion diameter (-▲-) compared with the calculated data (-●-).

This disagreement can be explained considering a hard-sphere model[8] and that the lamella surface consists of close-packed hydroxyl ions of radius $r_{OH} = a/2$, where a is the measured in-plane lattice parameter of ZnAl-Cl. This arrangement forms trigonal pockets on the surface in which the anion can be nested. The amount of nesting will depend on the halide ionic radius. The nesting degree (*nd*) of each anion can be obtained from the experimental data from the following equation:

$$nd = r_X - 1/2(d_x - t)$$

where r_X is the anion radius, d_X is the experimental distance of the dehydrated sample, t is the layer thickness (4.46 Å).

The maximum value of nesting can be obtained from simple geometric consideration (Fig. 10). The used equations are:

$$nd_{max} = [r_X + r_{OH}](1-\cos\theta) \qquad r_{OH} = 1.537 \text{ Å}$$

$$\theta = \arcsin\left[\frac{2}{\sqrt{3}\left(1+\dfrac{r_X}{r_{OH}}\right)}\right]$$

15
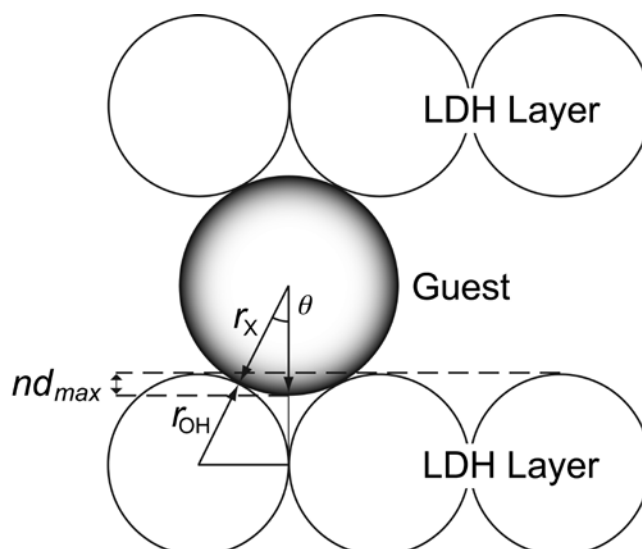
Fig. 10 Scheme of a halide ion (grey sphere) into trigonal pockets of the layer surface generated by closed-packed hydroxyl ions (white spheres). nd_{max} is the maximal nesting height.

The values of maximum nesting so obtained are relative to an ideal model in which the anion are located on the same plane and have the same nesting degree. A comparison between the nesting degree and the maximum nesting is reported in the Table 4.

Table 4 Comparison between the nesting degree and the maximum nesting in the dehydrated samples.

X	r	d (150°C)	nd	nd_{max}	$\%n$
F	1.33	6.30	0.41	0.62	66
Cl	1.81	7.30	0.39	0.50	78
Br	1.96	7.62	0.38	0.48	79
I	2.20	8.04	0.41	0.44	93

As expected, nd_{max} decreases with increasing the ionic radius, while the experimental nestings are not affected by the ionic radius. The agreement between the nesting degree and the maximum nesting is expressed as percentage of nesting and indicates the percentage of anion nested in the dehydrated samples. The experimental nesting represents an average value over all the sites occupied by the halides. The percentage of the halides nested increases with the dimension of the anion in agreement with Kamath.[20] The difference between the calculated (4.46 Å) and the observed (3.63 Å) lamellae thickness of 0.83 Å is twice than the experimental nd (average nd values for all the investigated anions = 0.40 Å). In Fig. 9 the basal spacing is plotted versus the ionic diameter. In this way the layer thickness is underestimated by an amount equal to twice the calculated nesting.

16

Structural data coming from Rietveld refinement of the halide exchanged LDH give some information on the interlayer distribution of the anions and can be used as term of comparison for the interpretation of the proposed nesting model.

In the 3-layer polytipic models of LDH (polytipes $3R_1$ and $3R_2$) the intensity ratio of *00l/002l* reflection is strictly dependent on the scattering factors and on the crystallographic sites of the intercalated anions which can affect the intensity owing to phase relationships between the brucitic layer and the interlayer region. In ZnAl-F and ZnAl-Br the position of the anions and of the water molecules was chosen according to the observed *003/006* intensity ratios (about a 1/2 for Br and 1/3 for F) which suggested a site with high degeneracy. For that reason the anions were placed in the *18h* Wickoff position and the occupancy factor was set to fixed values in agreement with the experimental formulas. Interlayer water molecules shared the same site according to previously reported LDH models with a full interlayer disorder. The occupancy of the water molecules was refined freely because the water content during the data collection was lower than the experimental values measured at controlled RH.

The positions of F^- and Br^- anions were let to refine freely along the plane until the best agreement of the calculated and observed intensities was reached. However, at the end of refinement, the position of Br^- and F^- differed considerably each other: in ZnAl-F the position of F^- and water molecules are thickened around the -3 axis (*6c* Wickoff position) whereas in ZnAl-Br the interlayer species are far away to this site, closer to the trigonal pockets made by the hydroxyl ions, thus suggesting a higher interlayer disorder. The same feature was also observed for ZnAl-I. As a matter of fact, if the Br^- (or I^-) was placed close or on the *6c* site the *003* reflection would have been completely extinct and, in our case, this is not observed.

This fact could be related to the different factor like the ionic radius and the electronegativity of the halide ion. The observed distances of F^- with the OH groups (*6c*) are about 2.86 - 2.9 Å, suggesting that F^- is able to make efficient H- bonds with the hydroxyl groups of the brucitic layer. This is in good agreement to recent papers in which the structures of several ZnAl-X (with X = Cl^-, Br^-, I^-, NO_3^- and CO_3^{2-}) were described by using both molecular dynamics simulations and XRPD.[18, 21]

The heavier and less electronegative Br^- and I^- anions are not able to form H- bonds with the OH groups and therefore they probably prefer to occupy more disordered positions upon the trigonal pocket, thus justifying the observed nesting model.

Rietveld plots for ZnAl-F and ZnAl-Br are reported in Fig. 11.

Table 5 Atomic positions, thermal and occupancy factors for ZnAl-F and ZnAl-Br

	x	y	z	U_{iso}	$Occ.$	$Mult.$
Sample ZnAl-F						
Zn	0	0	0	0.02(2)	0.61	3
Al	0	0	0	0.02	0.39	3
O(H)	0	0	0.3783(2)	0.02(2)	1.00	6
Ow	0.229(3)	0.457(5)	0.169(2)	0.06	0.06(1)	18
F	0.229(3)	0.457(5)	0.169(2)	0.06	0.065	18
Sample ZnAl-Br						
Zn	0	0	0	0.03(2)	0.61	3
Al	0	0	0	0.03	0.39	3
O(H)	0	0	0.3744(2)	0.03(2)	1.00	6
Ow	0.1254(8)	0.250(2)	0.1675(4)	0.06	0.05(1)	18
Br	0.1254(8)	0. 250(2)	0.1675(4)	0.06	0.065	18
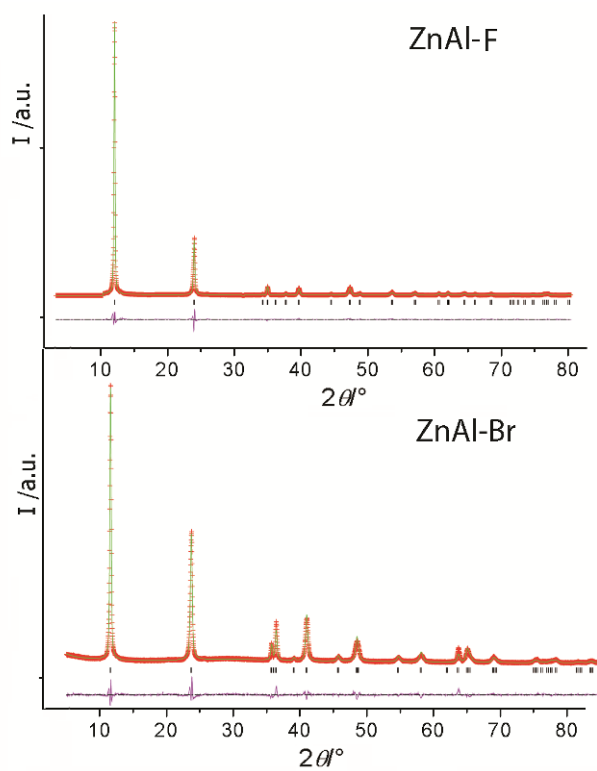
Fig. 11 Rietveld plots for ZnAl-F and ZnAl-Br

18

CONCLUSION

This work allowed to establish the following selectivity order of the ZnAl-LDH towards halides: F^- > Cl^- > Br^- > I^- . The ion exchange mechanism depends on the dimensions of the anions involved in the ion exchange process: when the dimensions are comparable the exchange goes on with the formation of a solid solution. On the contrary when the anions involved have different dimensions, the exchange goes on with a first order phase transition. The interlayer distance of the samples containing halides has been justified considering a nesting of the anions into the trigonal pockets of the LDH surface. The hard-sphere model allows to calculate the maximum nesting of the anions. The agreement between calculated and experimental nesting is better as the ion size increases, and it is an indication of the higher interlayer disorder of big halide ions. Rietveld refinement of the F^- and Br^- forms, together with the already reported I^- form, is in agreement with this observation, as the small F^- ions stay apart from the trigonal pocket being close to hydroxyl groups (6c site). In fact, the more electronegative F^- is able to form efficient H-bonds with hydroxyl groups. On the contrary Br^- and I^- occupied highly disordered sites, thus justifying the higher nesting degree with respect to F^-. Finally, it should also kept into account that the nesting model is calculated by using a rigid spheres model that cannot be properly applied to the soft and more polarisable anions like Br^- and I^-. This difference can justify the small discrepancy found for the calculated and the observed nesting values.

ACKNOWLEDGMENTS

REFERENCES

1 a) F. Trifirò, A. Vaccari and F. Cavani, *Catal. Today,* 1991, **11**, 173-301. b) *Layered Double Hydroxides: Present and Future*, ed. V. Rives, Nova Science Publishers: New York, 2001. c) W. Jones and S. P. Newman, *New J. Chem.,* 1998, **22**, 105-114. d) A. I. Khan and D. O'Hare, *J. Mater. Chem.,* 2002, **12,** 3191-3198. e) F. Leroux and C. Taviot-Guého, *J. Mater. Chem.*, 2005, **15**, 3628-3642. f) P. S. Braterman, Z. P. Xu and F. Yarberry, in *Handbook of layered Materials*; ed. Marcewl Dekker, New York, 2004, pp 373. (g) J. -M. Oh, T. T. Biswick and J. -H. Choy, *J. Mater. Chem.*, 2009, **19**, 2553-2563. (h) *Layered Double Hydroxides* in *Structure and Bonding;*

ed. X. Duan D. G. Evans, Springer-Verlag: Berlin, 2006, vol. 119. (i) *LDH in physical, chemical, bio-chemical and life sciences* in Developments in Clay Science – Volume 5B Handbook of Clay Science: Techniques and Applications, ed. F. Bergaya and G. Lagaly, 2013, vol. 5B.

2 a) R. Allmann, *Acta Cryst.,* 1968, **B24**, 972-977. b) H F.W. Taylor, *Miner. Mag.*, 1969, **37**, 338-384. c) U. Costantino, F. Costantino, F. Elisei, L. Latterini and M. Nocchetti, *PCCP*, 2013, **15**, 3254-3269.

3 (a) A.Vaccari, *Appl. Clay Sci.,* 1999, **14**, 161-244. (b) M. Turco, G. Bagnasco, U. Costantino, F. Marmottini, T. Montanari, G. Ramis and G. Busca, *J. Catal.*, 2004, **228**, 43-55. (c) T. Montanari, M. Sisani, M. Nocchetti, R. Vivani, M. Concepcion Herrera Delgado, G. Ramis, G. Busca and U. Costantino, *Catal. Today,* 2010, **152,** 104-109. (d) G. Busca, U. Costantino, T. Montanari, G. Ramis, C. Resini and M. Sisani *Int. J. Hydrogen Energy*, 2010, **35**, 5356–5366. c) A. Di Fronzo, C. Pirola, A. Comazzi, C. L. Bianchi, A. Di Michele, R. Vivani, M. Nocchetti, M. Bastianini, D. C. Boffito and F. Galli, *Fuel*, 2014, **119**, 62–69.

4 (a) U. Costantino, A. Gallipoli, M. Nocchetti, G. Camino, F. Bellucci and A. Frache, *Polym. Degrad. Stab*., 2005, **90**, 586-590. (b) U. Costantino, F. Montanari, M. Nocchetti, F. Canepa and A. Frache, *J. Mater. Chem.,* 2007, **17**, 1079-1086. (c) F. R. Costa, M. Saphiannikova, U. Wagenknecht and G. Heinrich, *Adv. Polym. Sci.*, 2008, **210**, 101-168. (d) G.G. Aloisi, F. Elisei, M. Nocchetti, G. Camino, A. Frache, U. Costantino and L. Latterini, *Mater. Chem. Phys.,* 2010, **123**, 372-377. (e) U. Costantino, M. Nocchetti, M. Sisani and R. Vivani, *Z. Kristallogr.,* 2009, **224**, 273-281. (f) U. Costantino, V. Bugatti, G. Gorrasi, F. Montanari, M. Nocchetti, L. Tammaro and V. Vittoria, *ACS Appl. Mater. Interfaces,* 2009, **1**, 668-677. (g) U. Costantino, M. Nocchetti, L. Tammaro and G. Gorrasi, in *Multifunctional and Nanoreinforced Polymers for Food Packaging,* ed. J. M. Lagaron, Woodhead Publishing: Cambridge, 2011, pp 43-85. (h) D.G. Evans and X. Duan, *Chem. Commun*., 2006, **5**, 485-496. (i) T. Posati, V. Benfenati, A. Sagnella, A. Pistone, M. Nocchetti, A. Donnadio, G. Ruani, R. Zamboni and M. Muccini, *Biomacromol.*, 2014, **15**, 158−168.

5 U. Costantino, V. Ambrogi, L. Perioli and M. Nocchetti, *Micropor. Mesopor. Mater.,* 2008, **107**, 149-160. b) *Clays and Health Clays in Pharmacy, Cosmetics, Pelotherapy, and Environmental Protection,* Special Issue of *Appl. Clay Sci.*, ed. M I. Carretero and G. Lagaly, 2007, vol. 36. c) J.-M. Oh, S.-J. Choi, G.-E. Lee, S.-H. Han and J.-H. Choy, *Adv. Funct. Mater.*, 2009, **19**, 1617-1624. d) E. Ruiz-Hitzky, P. Aranda, M. Darder and G. Rytwo, *J. Mater. Chem.*, 2010, **20**, 9306-9321. e) L. Perioli, V. Ambrogi, M. Nocchetti, M. Sisani and C. Pagano, *Appl. Clay Sci.*, 2011, **53**, 696–703. f) V. Ambrogi, V. Ciarnelli, M. Nocchetti, L. Perioli and C. Rossi, *Eur. J. Pharm.*

Sci., 2009, **73**, 285–291. g) M. Nocchetti, A. Donnadio, V. Ambrogi, P. Andreani, M. Bastianini, D. Pietrella and L. Latterini, *J. Mater. Chem. B*, 2013, **1**, 2383–2393.

6 S. Miyata, *Clays Clay Miner.*, 1983, **31**, 305-311.

7 R. P. Bontchev, S. Liu, J. L. Krumhansl, J. Voigt and T. M. Nenoff, *Chem. Mater.*, 2003, **15**, 3669-3675.

8 D. R. Hines, S. A. Solin, U. Costantino and M. Nocchetti, *Phys. Rev.B,* 2000, **61**, 11348-11538.

9 F. Okino and H. Touhara, in *Solid-State Supramolecular Chemistry: Two and Three-dimensional Inorganic Networks*, of *Comprehensive supramolecular Chemistry*, ed. G Alberti and T. Bein, Pergamon , Elsevier Science Ltd Press, Oxford, 1996, Vol. 7,ch. 2, pp 25-76.

10 G. Alberti and U. Costantino, in *Solid-State Supramolecular Chemistry: Two and Three-dimensional Inorganic Networks*, of *Comprehensive supramolecular Chemistry*, ed. G Alberti and T. Bein, Pergamon, Elsevier Science Ltd Press, Oxford, 1996, Vol. 7, ch. 1, pp 1-24.

11 a) A. M. Fogg, J. S. Dunn and D. O'Hare, *Chem. Mater.*, 1998, **10**, 356-360. b) N. Iyi, K. Kurashima and T. Fujita, *Chem. Mater.*, 2002, **14**, 583-589. c) Y. J. Feng, G. R. Williams, F. Leroux, C. Tavot-Gueho and D. O'Hare, *Chem. Mater.*, 2006, **18**, 4312-4318.

12 a) U. Costantino, S. Clementi, M. Nocchetti and R. Vivani, *Mol. Cryst. Liq. Cryst.,* 1998, **311**, 207. b) G. R. Williams, A. J. Norquist and D. O'Hare, *Chem. Mater.*, 2004, **16**, 975-981.

13 U. Costantino, F. Marmottini, M. Nocchetti and R. Vivani, *Eur. J. Inorg. Chem.*, 1998, **10**, 1439-1446.

14 (a) M. Bastianini, D. Costenaro, C. Bisio, L. Marchese, U. Costantino, R. Vivani and M. Nocchetti, *Inorg. Chem.*, 2012, **51**, 2560−2568. (b) G. M. Lombardo, G. C. Pappalardo, F. Punzo, F. Costantino, U Costantino and M. Sisani, *Eur. J. Inorg. Chem.,* 2005, **24**, 5026–5034.

15 P. Thompson, D.E. Cox and J.B. Hastings, *J. Appl. Cryst.*, 1987, **20**, 79-83.

16 R. D. Shannon, *Acta Crystallogr.,* 1976, **32**, 751-926.

17 J.A. Marinsky, in *Ion Exchange*, ed. Marcel Dekker, Inc., New York, 1966.

18 D. G. Costa, A. B. Rhoca, W. F. Souza, S. S. X. Chiaro and A. A. Leitao, *Appl. Clay Sci.*, 2012, **56**, 16-22.

19 N. Iyi, K. Fujii, K. Okamoto and T. Sasaki, *Appl.Clay Sci.,* 2007, **35**, 218-227.

20 S. V. Prasanna, P. V. Kamath and C. J. Shivakumara, *Colloid Interface Sci.,* 2010, **344**, 508-512.

21 G. M. Lombardo, G. C. Pappalardo, F. Costantino, U. Costantino and M. Sisani, *Chem. Mater.,* 2008, **20**, 5585–5592.
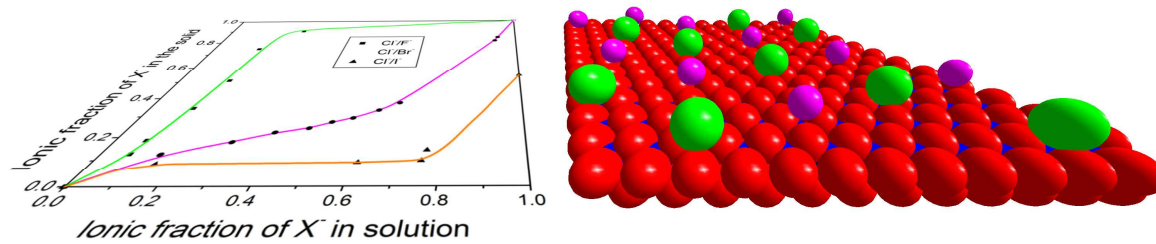
The selectivity towards halides and mechanism of ion exchange of the ZnAl-LDH in chloride form ($X^- = F^-$, Br^-, I^-) was investigated by ion exchange isotherms Cl^-/X^-.